Ultrastructural, Immunofluorescence, and RNA Evidence Support the Hypothesis of a "New" Virus Associated With Kawasaki Disease

Anne H. Rowley,[1,2] Susan C. Baker,[3] Stanford T. Shulman,[1] Kenneth H. Rand,[4] Maria S. Tretiakova,[5] Elizabeth J. Perlman,[6] Francesca L. Garcia,[1] Nuzhath F. Tajuddin,[3] Linda M. Fox,[7] Julia H. Huang,[1] J. Carter Ralphe,[8] Kei Takahashi,[9] Jared Flatow,[10] Simon Lin,[10] Mitra B. Kalelkar,[11] Benjamin Soriano,[12] and Jan M. Orenstein[13]

[1]Department of Pediatrics and [2]Department of Microbiology–Immunology, Feinberg School of Medicine, Children's Memorial Hospital, Northwestern University, Chicago, [3]Department of Microbiology and Immunology, Stritch School of Medicine, Loyola University, Maywood, Illinois; [4]Department of Pathology, Immunology, and Laboratory Medicine, University of Florida College of Medicine, Gainesville, Florida; [5]Department of Pathology, Division of Biological Sciences, University of Chicago, [6]Department of Pathology, Feinberg School of Medicine, Children's Memorial Hospital, Northwestern University, Chicago, [7]Department of Pathology, Stritch School of Medicine, Loyola University, Maywood, Illinois; [8]Department of Pediatrics, University of Wisconsin School of Medicine and Public Health, Madison; [9]Department of Pathology, Toho University School of Medicine, Tokyo, Japan; [10]Clinical and Translational Sciences Institute, Feinberg School of Medicine, Children's Memorial Hospital, Northwestern University, Chicago; [11]Office of the Medical Examiner, Cook County Institute of Forensic Medicine, Chicago, Illinois; [12]Department of Pathology and Laboratory Medicine, University of Wisconsin School of Medicine and Public Health, Madison; and [13]Department of Pathology, George Washington University Medical Center, Washington, DC

Background. Intracytoplasmic inclusion bodies (ICI) have been identified in ciliated bronchial epithelium of Kawasaki disease (KD) patients using a synthetic antibody derived from acute KD arterial IgA plasma cells; ICI may derive from the KD etiologic agent.

Methods. Acute KD bronchial epithelium was subjected to immunofluorescence for ICI and cytokeratin, high-throughput sequencing, and transmission electron microscopy (TEM). Interferon pathway gene expression profiling was performed on KD lung.

Results. An intermediate filament cytokeratin "cage" was not observed around KD ICI, making it unlikely that ICI are overproduced or misfolded human protein aggregates. Many interferon-stimulated genes were detected in the bronchial epithelium, and significant modulation of the interferon response pathway was observed in the lung tissue of KD patients. No known virus was identified by sequencing. Aggregates of virus-like particles (VLP) were detected by TEM in all 3 acute KD patients from whom nonembedded formalin-fixed lung tissue was available.

Conclusions. KD ICI are most likely virus induced; bronchial cells with ICI contain VLP that share morphologic features among several different RNA viral families. Expedited autopsies and tissue fixation from acute KD fatalities are urgently needed to more clearly ascertain the VLP. These findings are compatible with the hypothesis that the infectious etiologic agent of KD may be a "new" RNA virus.

Kawasaki disease (KD) is a systemic vasculitis of young childhood that most significantly affects the coronary arteries. Although fatality rates are relatively low in countries attuned to the signs and symptoms and thus the diagnosis, the worldwide mortality and morbidity rates are unknown. Although the cause is unknown, clinical and epidemiologic data support the hypothesis of a ubiquitous etiologic agent that likely causes an inconsequential respiratory infection in the vast majority of children but disseminates and results in KD in a subset of children who are genetically predisposed [1]. An antigen-driven IgA immune response was detected in the walls of coronary and other arteries in the weeks following the onset of illness, leading to the hypothesis that the etiologic agent is microbial [2]. The beneficial or deleterious effect of the IgA antibodies remains to be ascertained. Synthetic versions of the IgA antibodies detect intracytoplasmic inclusion

Received 8 April 2010; accepted 23 July 2010.

Potential conflicts of interest: none reported.

Presented in part: Pediatric Academic Societies' Meeting, Vancouver, British Columbia, Canada, 1–4 May 2010.

Reprints or correspondence: Anne H. Rowley, MD, Northwestern University Feinberg School of Medicine, 310 E Superior St., Morton 4-685B, Chicago, IL 60611 (a-rowley@northwestern.edu).

The Journal of Infectious Diseases 2011;203:1021–30

1537-6613/2011/2037-0001$15.00
DOI: 10.1093/infdis/jiq136

bodies (ICI) consistent with aggregates of viral protein and RNA in the apical region of ciliated epithelial cells of predominantly mid-sized bronchi of 85% of children with fatal KD, but not of infant controls [3–5]. With experience, the ICI can also be identified by light microscopy in hematoxylin-eosin stain sections.

Cytoplasmic inclusions can be seen in a variety of virus and bacterial infections. They can also result from overproduced or misfolded aggregates of human proteins (ie, "aggresomes"[6]) in chronic neurodegenerative diseases such as Alzheimer's [7]. A primary feature of aggresomes is that they are surrounded by an intermediate filament "cage" [7]. Bacterial inclusion bodies contain bacterial forms that reflect their life cycle [8], in contrast to KD ICI, which are homogeneous.

To determine whether the ICI seen in KD have a cage characteristic of an aggresome, we performed colocalization experiments using KD synthetic antibody plus an antibody to human cytokeratin, the intermediate filament present in bronchial epithelium [9]. To determine the nature of the RNAs in the apical cytoplasm of bronchial epithelium containing ICI, we performed laser-capture microdissection, isolated RNA, and synthesized and sequenced complementary DNA (cDNA) using high-throughput methods. We performed real-time reverse transcription–polymerase chain reaction (RT-PCR) for selected genes on lung RNA from KD patients and infant controls.

We analyzed the bronchial epithelium of formalin-fixed, non–paraffin embedded lung tissue from autopsies of 3 KD patients by transmission electron microscopy (TEM) to determine if any microbial forms could be observed in specimens containing ICI.

METHODS

Patients

The KD and control lung tissues were from cases not included in our previous reports [3–5, 10] (Table 1), although we used lung tissues from 1 KD case reported previously [3] for the real-time polymerase chain reaction (PCR) analysis as described below.

Antibodies and Reagents

We prepared KD synthetic antibody J as previously described [3, 4]. We obtained pan-cytokeratin antibody from ScyTek Laboratories. ImageIT-FX Signal Enhancer, AlexaFluor 568 conjugate, and Prolong Gold Mounting media with DAPI were from Invitrogen. TSA-Fluorescein was from Perkin Elmer. ABC reagent was from Vector.

Immunohistochemistry

We performed immunohistochemistry using KD synthetic antibody J and control synthetic antibody, as previously described [3–5].

Laser-capture Microdissection and 454 Sequencing

We performed laser-capture microdissection of the apical cytoplasm of ciliated bronchial epithelial cells containing ICI on six 5-micron sections of formalin-fixed, paraffin-embedded lung from KD patient 2 at the University of Chicago using a Leica AS Laser Microdissection microscope. We first laser-ablated nuclei. We used proteinase K to digest the tissue, and we isolated the RNA using Trizol (Invitrogen), followed by treatment with DNase. We prepared cDNA using the Transplex Whole Transcriptome Amplification system (Sigma-Aldrich). We performed 454/FLX sequencing at the Interdisciplinary Center for Biotechnology Research of the University of Florida at Gainesville.

Bioinformatics Analysis

After masking for 454 and Transplex primer sequences, we performed basic local alignment search tool (BLAST) analysis with default parameters against human and nucleotide databases. We listed human messenger RNAs (mRNAs) according to the frequency of hits. We mined the data for matches to known viral sequences.

Immunofluorescence Assays

We freed sections from paraffin, rehydrated them, subjected them to antigen retrieval in 10 mM sodium citrate, and treated them with hydrogen peroxide as previously described [3, 4], except we applied Image IT signal enhancer for 30 minutes just prior to hydrogen peroxide treatment. We blocked sections with 5% goat serum containing 3% Triton X-100, and incubated them with biotinylated KD antibody J [4] at 10 μg/mL and prediluted pan-cytokeratin antibody for 1 hour at room temperature. We then incubated slides with ABC reagent and Alexafluor 568 goat anti–mouse IgG (1:1000), washed them, and incubated them with TSA amplification reagent according to the manufacturer's instructions. We then washed, mounted, and incubated slides in the dark for 24 hours before examining them under a Zeiss LSM 510 laser scanning microscope.

Real-time Polymerase Chain Reaction

We prepared RNA from formalin-fixed, paraffin-embedded blocks of whole lung from control 1, controls 5–8, KD patients 1 and 2 (this study), and 1 KD patient reported in a prior study [3] using a FFPE RNA extraction kit (Qiagen). The therapy received by patient KD 1 was intravenous immunoglobulin (IVIG), solumedrol, and infliximab; patient 2 had received IVIG and solumedrol. The third patient [3] used in real-time PCR analysis was not diagnosed prior to death; he therefore did not receive any KD therapy. RNA was treated with Turbo DNase (Ambion), and purified using the MinElute RNA purification kit (Qiagen). cDNA was prepared from .3 μg of RNA using an RT^2 FFPE PreAmp cDNA synthesis kit and primer mix for the interferon α, β response (SA Biosciences). We evaluated samples for expression of ribosomal RNA and human genomic DNA contamination (by RT^2 QC PCR array) and subjected to real-time PCR analysis using an interferon alpha, beta response PCR array (SA Biosciences) on a Biorad Opticon 2 Real Time PCR Detector. Statistical analysis

Table 1. Clinical Data on Kawasaki Disease Patients and Controls

Patient and Ethnicity (if known)	Age	Gender	Duration of KD Illness	ICI	Cause of Death
KD1 Hispanic	3 mo	M	3–4 wk	Yes	Ruptured common iliac artery aneurysm with massive hemorrhage. Aneurysms of coronary, axillary, brachial, iliac arteries, aorta.
KD2 Caucasian	3 mo	M	15 d	Yes	Bowel infarction due to mesenteric arteritis and thrombosis. Aneurysms of coronary, mesenteric, axillary, renal, intervertebral, femoral arteries
KD3 Japanese	3 y	M	16 d	Yes	Rupture of LAD coronary artery aneurysm
KD4 Greek	2 yrs	F	4 mo	Yes	Myocardial infarction from thrombosis/ stenosis of coronary artery aneurysm.
Control 1	5 wk	M	N/A	No	Demyelinating neurologic disease
Control 2	3 wk	M	N/A	No	Tetrology of Fallot
Control 3	1 mo	F	N/A	No	Supraventricular tachycardia
Control 4	3 mo	M	N/A	No	Malrotation, volvulus
Control 5	2 mo	F	N/A	No	Malignant glioma
Control 6	1 mo	M	N/A	No	Anoxic ischemic encephalopathy
Control 7	10 d	M	N/A	No	Metabolic disease, seizures
Control 8	5 mo	M	N/A	No	Metabolic leukodystrophy
Control 9	3 wk	F	N/A	No	Sudden infant death syndrome
Control 10	6 d	M	N/A	No	Anoxic ischemic brain damage

NOTE. ICI, intracytoplasmic inclusion bodies detected in the bronchial epithelium by immunohistochemistry using synthetic antibody J; N/A, not applicable.

was performed using PCR array data analysis software (SA Biosciences).

Transmission Electron Microscopy

We performed transmission electron microscopy (TEM) on formalin-fixed tissue from patients 1, 2, and 3 that was further fixed with 2.5% neutral buffered glutaraldehyde, postfixed with osmium tetroxide, processed through graded ethanol and propylene oxide, and embedded in Spurr's epoxy. Semithin (1 μm) plastic sections were cut with a glass knife and stained with methylene blue/azure II/basic fuchsin trichrome stain for plastic section light microscopy. We selected blocks for TEM based on the presence of ciliated epithelium containing ICI, thinned them with a diamond knife, stained them with uranyl acetate and lead citrate, and examined them on a LEO EM10 TEM operating at 60 kV.

RESULTS

Immunohistochemistry Confirms the Presence of Intracytoplasmic Inclusion Bodies in Kawasaki Disease But Not in Control Patients

Immunohistochemistry using KD synthetic antibody J revealed the presence of ICI in cilated bronchial epithelium in all 4 KD cases but not in the 10 infant controls; nonciliated bronchial cells did not contain ICI. ICI were consistent with those seen in the other KD cases that have previously been reported [3–5]; we observed no intranuclear inclusions. Results using control synthetic antibody were negative in KD patients and controls.

Kawasaki Disease Intracytoplasmic Inclusion Bodies Were Not Surrounded by an Aggresome-like Intermediate Filament "Cage"

To determine whether KD ICI had an aggresome-like intermediate filament cage, we incubated lung sections from KD patients 2 and 4 with KD synthetic antibody J and a pan-cytokeratin antibody, and examined them by immunofluorescence. The distribution of cytokeratin in KD bronchial epithelium was similar to that seen in control infants (Figure 1A). Cytokeratin cages were not evident around KD ICI in either patient (Figures 1B, 1C), suggesting that the ICI do not represent aggregates of misfolded or overproduced human protein.

Interferon-stimulated Genes were Detected in Kawasaki Disease Bronchial Epithelium Containing Intracytoplasmic Inclusion Bodies

Of a total of 411,561 reads obtained by 454 sequencing of the laser-captured tissue from KD patient 2, most were human ribosomal RNA and DNA sequences; approximately 14,500 human mRNAs were identified (Supplemental table 1). A comparison of the transcriptome of KD ciliated bronchial epithelium to the transcriptome of control adult bronchial epithelium [11] revealed many genes expressed at comparable levels, such as CD24, tetraspanin 1, ezrin, secretoglobin, alpha actinin 1, and mucin 5AC. A striking number of interferon-induced genes were detected

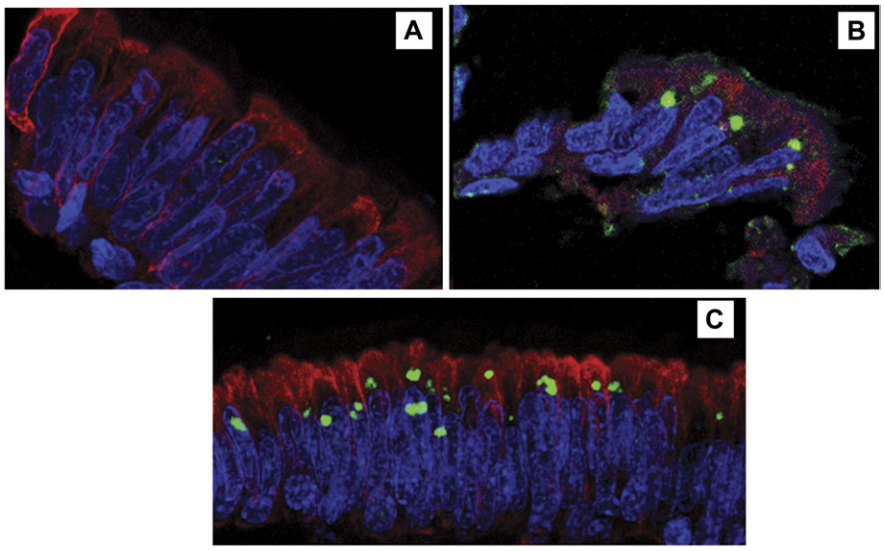

Figure 1. Confocal immunofluorescence for Kawasaki Disease intracytoplasmic inclusion bodies (green) and cytokeratin (red) in formalin-fixed, paraffin-embedded cilated bronchial epithelium. *A*, Compressed Z-stack image of bronchial epithelium of control 8, showing cytoplasmic expression of cytokeratin and absence of ICI. *B*, single plane image of KD bronchial epithelium from Kawasaki disease (KD) patient 2. Intracytoplasmic inclusion bodies (ICI) are roughly spherical and reside just above nuclei; cytokeratin is in the supranuclear cytoplasm but does not form a "cage" around the ICI. *C*, Compressed Z-stack image of bronchial epithelium of KD patient 3, showing that cytokeratin is expressed in the cytoplasm but does not form a "cage" around the ICI. Some cells have more than 1 ICI and some ICI are somewhat irregular in shape. Nuclei are stained with 4′,6-diamidino-2-phenylindole (blue). Original magnification: x400 for all panels.

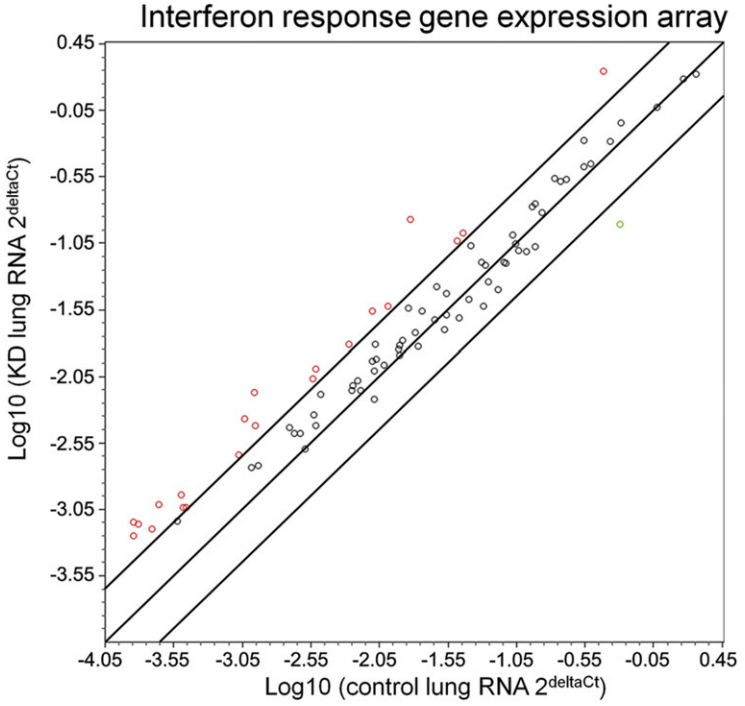

Gene Symbol	Fold Regulation
BST2	2.7
CNP	3.4
GBP2	3.3
GCH1	6.2
HLA-C	9.0
HLA-E	2.8
HLA-F	3.6
HLA-G	5.0
HSPA1L	4.4
IFITM1	2.9, p=.040
IFITM2	4.6, p=.002
IFNA2	3.9
IFNA4	3.2
IFNAR1	4.6
IRF7	3.5
ISG15	2.7
ISG20	2.9
MAL	2.8
MX2	2.9
SAMSN1	2.9
SHFM1	4.5
TNFSF10	-4.1, p=.001

Figure 2. Real-time polymerase chain reaction analysis of interferon-stimulated genes in acute Kawasaki Disease and control lung. Interferon α, β response polymerase chain reaction array revealed 21 genes upregulated (>2.5-fold) in Kawasaki disease when compared with that of control lung; IFITM1 and IFITM2 were statistically significantly upregulated. 1 gene on the array, TNFSF10, was significantly downregulated and was the only gene downregulated >2.5-fold. Lines indicate boundaries for 2.5-fold up- or downregulation of genes in this pathway. Genes upregulated are indicated in red, and downregulated genes are in green.

Table 2. Interferon-stimulated Genes Detected Among 14,500 mRNAs in Acute Kawasaki Disease Ciliated Bronchial Epithelium Containing Intracytoplasmic Inclusion Bodies

Entrez Gene ID	Gene Name	Number of Hits
ADAR	Adenosine deaminase, RNA-specific	9
LGALS3BP	Lectin, galactoside-binding, soluble, 3 binding protein	6
HLA-C	Major histocompatibility complex, class I, C	6
UBA7 (UBE1L)	Ubiquitin-like modifier activating enzyme 7	6
CREBBP	CREB binding protein	5
NAMPT	Pre-B-cell colony enhancing factor 1	5
EP300	EE1A binding protein p300	5
JAK1	Janus kinase 1	5
UBA6 (UBE1L2)	Ubiquitin-like modifier activating enzyme 6	4
TAP1	Transporter 1, ATP-binding cassette, subfamily B	4
ITGA2	Integrin, alpha 2 (CD49B)	4
APOL6	Alipoprotein L, 6	3
ZC3HAV1	Zinc-finger CCCH-type, antiviral 1	2
PSME1	Proteosome activator subunit 1	2
HMGCS1	3-hydroxy-3-methylglutaryl-Coenzyme A synthase 1	2
DHX58	DEXH box polypeptide 58	2

NOTE. Each Appears ⩽ once in 150,000 mRNAs in the adult bronchial epithelial transcriptome [11].

among the KD mRNAs but not reported in the bronchial epithelial transcriptome of adult controls (Table 2). Interferon-stimulated gene expression is relatively toxic and generally short-lived within cells [12], and gene expression databases indicate that interferon-induced genes such as adenosine deaminase, RNA-specific, appear to be expressed at lower levels in infants compared with that of adults (http://www.ncbi.nlm.nih.gov/UniGene/EST-ProfileViewer.cgi?uglist=Hs.12341, last accessed 24 January 2011), increasing the likely significance of this finding.

Interferon-stimulated Gene Expression in Kawasaki Disease Lung

To further investigate expression of interferon-stimulated genes in acute KD, real-time PCR analysis was performed on RNA isolated from formalin-fixed, paraffin-embedded lung tissue from acute KD patients and infant controls. The RNA quality isolated from multiple KD and control lung blocks was assessed by evaluating expression of housekeeping genes and genomic DNA contamination; only a subset of samples were adequate for further evaluation (KD n = 3, infant control n = 5). Using an interferon alpha, beta response array, we evaluated the expression of 84 genes normalized to expression of the housekeeping gene ribosomal protein L13a. Within this pathway, 21 genes were upregulated >2.5-fold in KD compared with that of control lung, with statistically significant upregulation of interferon induced transmembrane protein 1 (*IFITM1*, $P = .04$) and interferon-induced transmembrane protein 2 (*IFITM2*, $P = .002$) (Figure 2). Only 1 gene was downregulated: tumor necrosis factor (ligand) superfamily member 10 (*TNFSF10*, $P = .001$). These results indicate that there is significant modulation of the interferon response pathway in KD lung.

No Known Virus Was Identified in Laser-captured Acute Kawasaki Disease Ciliated Bronchial Epithelium by High-throughput Sequencing

Of the 411,561 reads obtained by 454 sequencing, BLAST analysis did not reveal any known viral sequences in ICI. The 1006 sequence reads present in the KD sample but without a match in Genbank will require further analysis.

Virus-like Particles Were Observed in Ciliated Epithelium From Patients With Intracytoplasmic Inclusion Bodies

We performed TEM on ICI-containing bronchi from 3 formalin-fixed, non-paraffin-embedded lung specimens. Because there was only poorly preserved paraffin-embedded tissue available from case 4, TEM was not performed. The ultrastructural study focused particularly, but not exclusively, on the ciliated bronchial epithelial cells that contained ICI. Multiple pieces of lung tissue (up to 25) were processed into plastic and screened for bronchi containing ICI. At least 2 positive blocks were thinned and 2 grids prepared from each were thoroughly examined, from low through high magnification.

Although cases 2 and 3 had ample ICI in the plastic sections examined by LM, they were relatively uncommon in the available sections from case 1. Signs of poor cellular preservation, typical of epithelium from autopsy material, were present (eg, dissociation and sloughing of epithelial cells, membrane fragmentation and even dissolution, cytosolic wash-out, and organelle swelling and rupture). We observed no intranuclear inclusions. Despite the poor preservation, we identified clusters of virus-like particles (VLP) in all 3 cases.

The VLP in case 1 were not found in direct association with the few ICI (Figure 3A) found by TEM, but they were observed concentrated in several ciliated bronchial epithelial cells (Figure 3B–D). Figures 3C and 3D show images of the 50 nm VLP. They were either homogeneously electron dense or contained a lighter central "core" (Figure 3C). A few appeared to be hexagonal (Figure 3D), whereas 1 VLP could be interpreted as having been fixed while in the process of budding (Figure 3D). There was only a suggestion that the VLP might have had a unit membrane. Some VLP had what might have been a corona of "spikes" (Figures 3C, 3D). Because of the poor preservation, it was difficult to identify the exact cytoplasmic location of the VLP. Sometimes

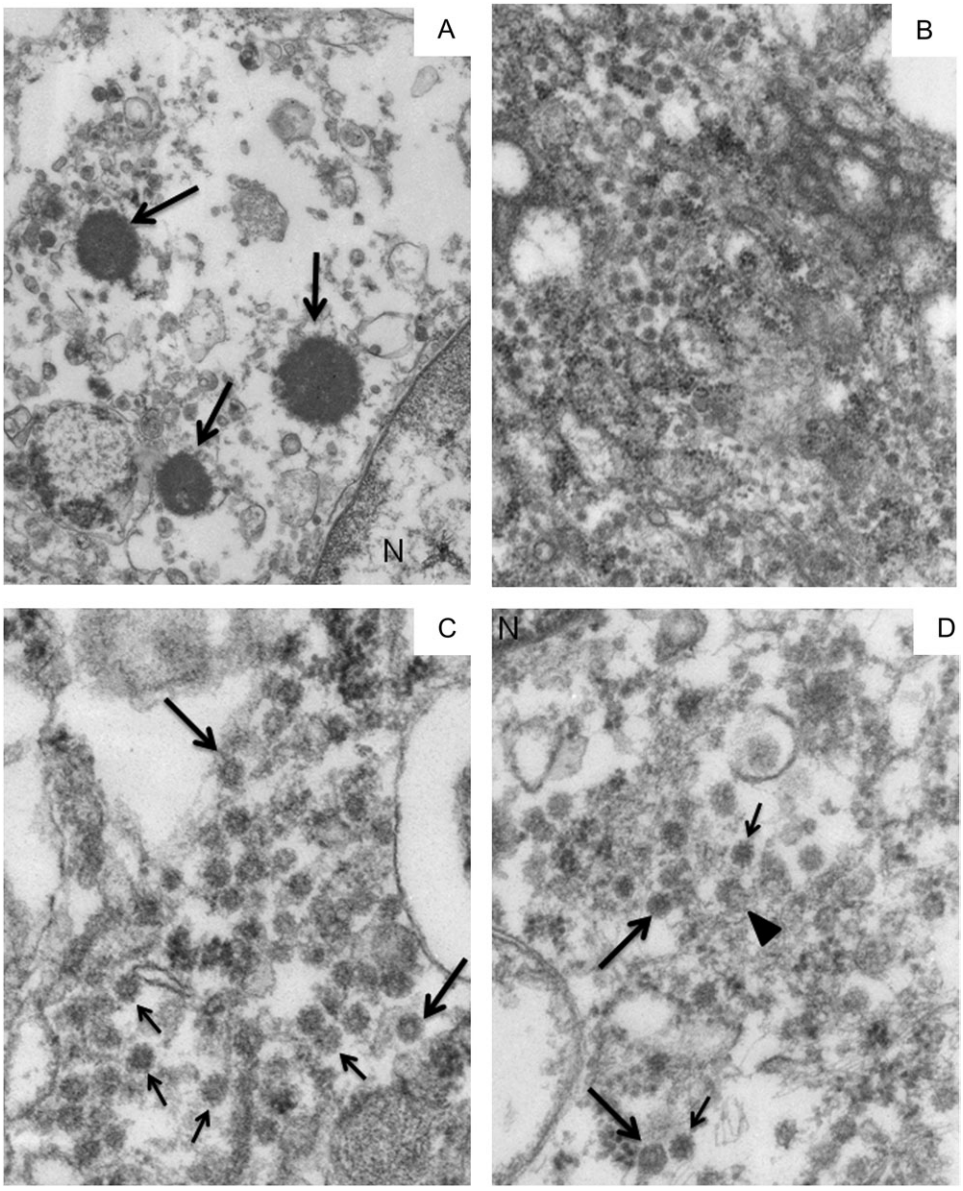

Figure 3. Transmission electron microscopy of 3 intracytoplasmic inclusion bodies in 1 cell and of virus-like particles in 3 different bronchial epithelial cells in Kawasaki Disease Patient 1. *A,* Although most of the cytoplasm is washed out, three, small round, electron-dense supranuclear intracytoplasmic inclusion bodies (ICI) are preserved (arrows). They are surrounded by pleomorphic vesicles that could not be further delineated. *B,* A medium magnification electron micrograph of a large field of cytoplasmic virus-like particles (VLP) in a second cell. *C,* A cluster of identical-appearing VLP in a third cell. Some VLP have central lighter ''cores'' (eg, large arrows), whereas others may have ''spikes'' (eg, small arrows). *D,* Another cluster of electron-dense VLP is seen in a fourth cell. 2 particles appear to have a hexagonal outline (large arrows), another may have been caught in the act of budding (arrowhead), and several have what may be a corona of ''spikes'' (eg, small arrows). A mitochondrion in the lower left field is almost unrecognizable, an indication of the poor organelle preservation. Original magnification: x26,000 for panel A; x50,000 for panel B; x105,000 for panels C, D.

their background was clear, suggesting the possibility that they might have been in vacuoles, endoplasmic reticulum, or Golgi.

Case 2 had typical KD ICI, electron-dense with a regular surface (Figure 4A). 1 ICI was intimately associated with many 50 nm VLP that were photographed in multiple sections (Figure 4B, 4C, 4D). The ICI were clearly in the supranuclear Golgi/RER zone (Figure 4B). This ICI, like many others in the specimens, had a more irregular shape and were of lower electron-density than usual, including those seen in previously studied formalin-fixed, paraffin-embedded lung tissue from 15 KD cases [for examples, see 4]. Case 2 also had typical, more regular, electron dense ICI (Figure 4A). The VLP had a unit membrane surrounding a ''gray''-staining interior (Figures 4C,4D). Rarely, there was a denser central ''core''-like structure. Most VLP were round to oval and rarely had a straight side. Some VLP appeared to be at least partially encompassed by 1 or 2 similar unit membranes. This ICI,

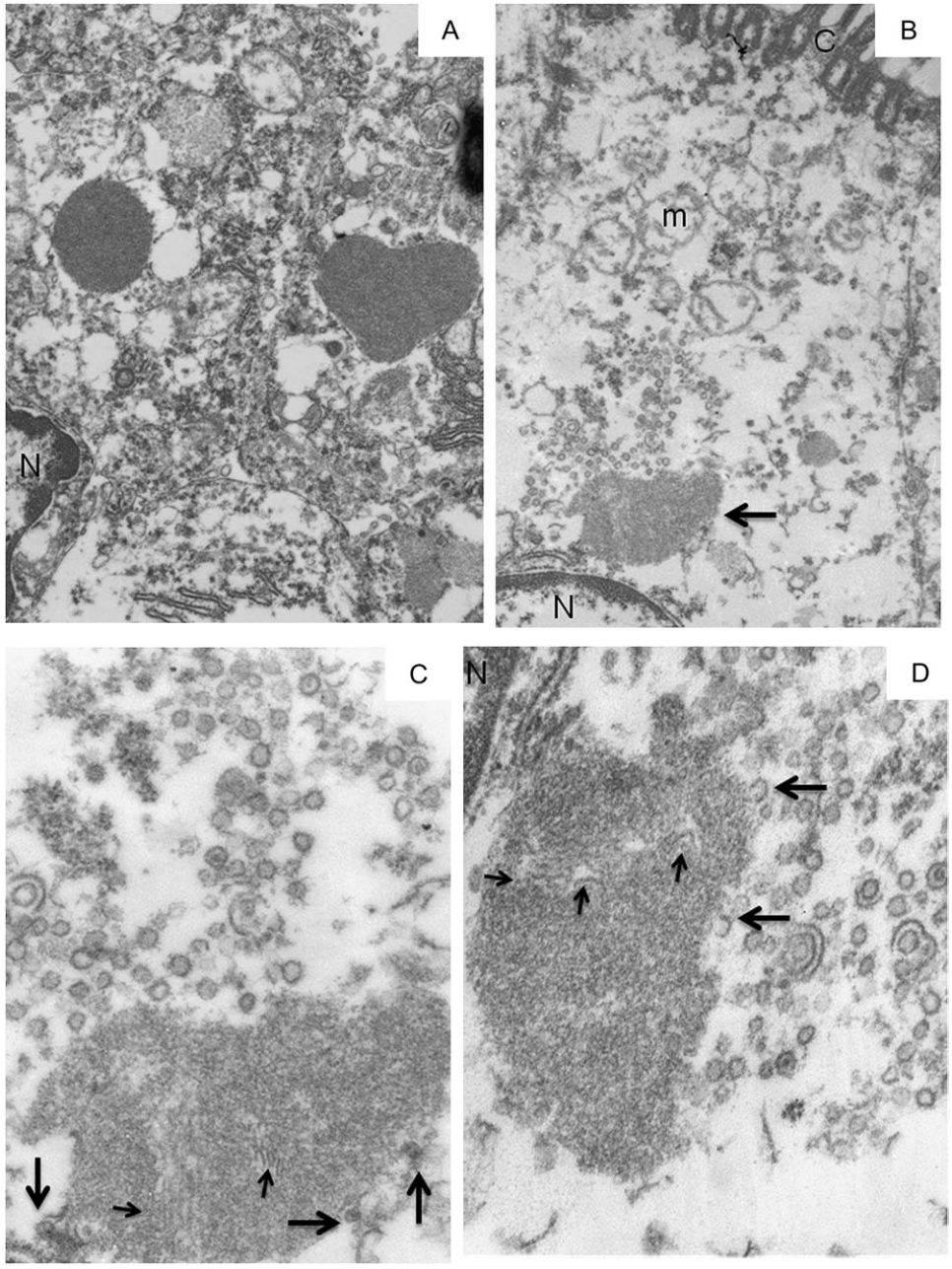

Figure 4. Transmission electron microscopy of intracytoplasmic inclusion bodies and virus-like particles in Kawasaki Disease Patient 2. *A*, 2 Intracytoplasmic Inclusion Bodies (ICI) of typical "mature" electron density and crisp outlines are in adjacent, better preserved ciliated cells; 1 ICI is oval, whereas the other has an unusual heart shape. *B*, An irregular, lighter-staining, supra-nuclear ICI (arrow) is partly surrounded by virus-like particles (VLP). Most of the cytoplasm is washed out and the mitochondria are severely damaged. *C*, A higher magnification of the VLP above the ICI in *B*. The ICI contains filaments of similar thickness to the VLP membrane (eg, small arrows); 3 VLP are intimately associated with the surface of the ICI (large arrows). *D*, At a different level of the same ICI, the VLP appear mostly empty, save for a rare denser "core". "Extra" unit membranes surround 2 VLP; 2 incomplete VLP appear associated with the surface of the ICI (eg, large arrows). Additional filaments are seen within the ICI (small arrows). Part of the nucleus (N) and a single profile of rough endoplasmic reticulum are seen in the upper left field. Note: N = nucleus, C = cilia, m = mitochondrion. Original magnification: x 26,000 for panels A, B; x105,000 for panels C, D.

as well as others in the specimen, was inhomogeneous and contained 20 nm thick filamentous or membranous structures, which were occasionally in aggregates. A few "incomplete" VLP were intimately associated with the edge of the ICI (Figure 4C, 4D).

In case 3, variably electron-dense ICI were abundant (Figure 5A). Some contained 20 nm filaments that were up to 150 nm in length. Near typical ICI several cells contained smaller, less well-defined, less electron-dense inclusions, variably containing 20 nm filaments up to 240 nm in length (Figure 5A). Their appearance suggested that they were likely developing ICI (ie, "premature ICI"). In 1 ciliated bronchial epithelial cell, there was a large cluster of haphazardly

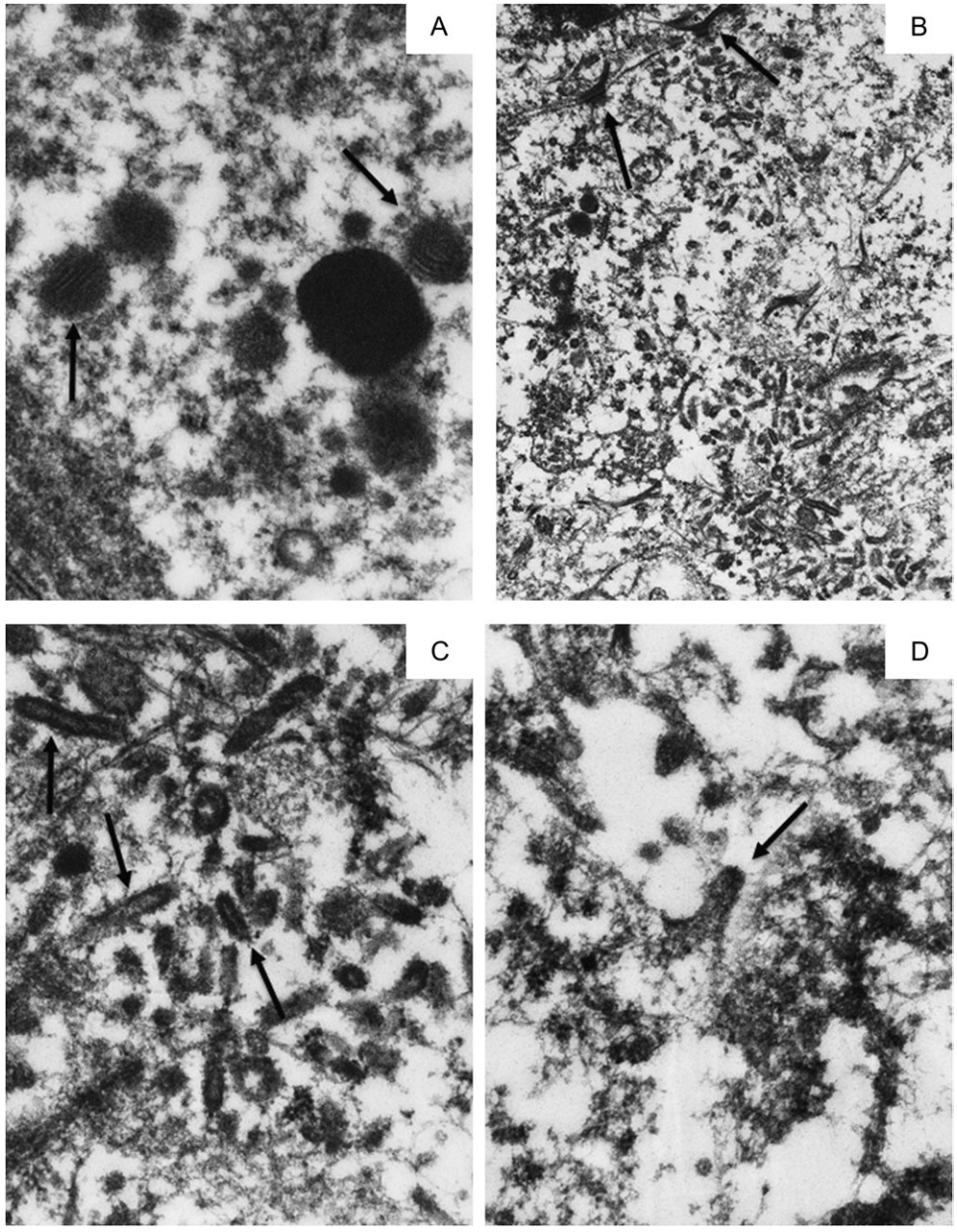

Figure 5. Transmission electron microscopy of intracytoplasmic inclusion bodies and virus-like particles in Kawasaki Disease Patient 3. *A*, A typical electron-dense, smooth-surfaced intracytoplasmic inclusion body (ICI) is surrounded by 5 poorly delineated, lighter staining ''pre-ICI''; 2 contain 20 nm wide filaments (arrows); 2 pre-ICI appear to be fusing, whereas 2 others are closely associated with the ICI. *B*, Desmosomes (arrows) join 2 epithelial cells. A large area of the cytoplasm contains haphazardly arranged virus-like particles (VLP) and tufts of cytokeratin. *C*, The VLP have rounded ends and lighter-staining cores (eg, arrows). *D*, This VLP, and others not shown, appear to have been fixed during the act of budding from a membrane that can't be identified. Original magnification: x80,000 for panel A; x26,000 for panel B; x105,000 for panels C, D.

arranged, rod/bullet-shaped VLP that had a more electron lucent core (Figures 5B,5C). These VLP were encased in a unit membrane, but it was not possible to ascertain whether they had surface spikes. They were approximately 80 nm wide and could be up to 400 nm long. We observed several apparently budding forms with a clear unit membrane, but the membranes from which they were budding were not preserved and could not be identified (Figure 5D).

DISCUSSION

Clinical and epidemiologic features are consistent with a viral etiology for KD, but no known virus has been convincingly associated [1]. ICI were identified in KD tissue following the discovery that IgA plasma cells that are oligoclonal, ie, antigen-driven [2, 10], are present in inflamed KD coronary arteries, likely targeting an infectious agent. Synthetic versions of these

oligoclonal antibodies were prepared, which identified an antigen in KD autopsy tissues [3, 4]. Light and electron microscopic studies localized the antigen to ICI in both ciliated bronchial epithelium and to a subset of macrophages in lungs, spleen, and lymph nodes [3, 4]. Because a single monoclonal antibody detected ICI in 85% of KD fatalities of varying ethnicity and origin, it followed that the same antigen should be present in the vast majority of KD cases [3–5]. ICI were not detected in 20 infant controls (including the 10 reported here), but were detected in 25% of autopsy material from anonymous older childhood and adult controls [5]. The possibility exists that KD results from a pulmonary infection by an RNA virus that is widely distributed in the world population and in susceptible children can disseminate intravascularly, possibly in macrophages, leading to the development of KD vasculitis, most significantly of the coronary arteries [5]. ICI can be considered as a possible ''footprint'' of the viral infection that may persist indefinitely [5].

High-throughput sequencing of KD laser-captured bronchial epithelium containing ICI revealed the expression of many interferon-stimulated genes, in keeping with a cellular response to a viral infection. Real-time PCR analysis confirmed their presence in KD lung, particularly *IFITM1* and *IFITM2*. A caveat of the study is that the 3 KD patients examined by real-time PCR analysis received 3 therapies, 2 therapies, and no therapy; it is possible that this could have affected the results, although it seems more likely that anti-inflammatory therapies might have dampened rather than upregulated interferon responses.

A significant consideration was whether any normal cellular structures might have the VLP appearances described here, especially those in case 1 (eg, clathrin-coated vesicles [CCV]). CCV aggregates of such large size have never previously been observed in decades of experience performing TEM on surgical, autopsy, or experimental lung specimens (JMO). CCV are derived from the plasma membrane endocytic/micropinocytic system, are more variable in size than the VLP and contain proteins or other endocytized substances. The clathrin coating is bristle-like and CCV are spherical, without a hint of a flat surface such as a hexagonal configuration. Once in the cytoplasm, CCV shed their clathrin, which is then recycled to the plasma membrane.

In case 2, it was not possible to determine whether the ''incomplete'' VLP intimately associated with the ICI were fusing with or budding from the ICI, or whether the other ''atypical'' appearing ICI in this specimen were in a formative or ''immature'' stage, with VLP either being ultimately added to the maturing ICI or adding some component to the ICI. The presence of VLP-like membranous material in the ICI suggests that the VLP were more likely fusing with the ICI than budding. In case 3, we observed ''pre-ICI'' that also had the appearance of ''immature'' ICI.

Over several decades of performing TEM on a plethora of diagnostic and research specimens (JMO), collections of such VLP structures have not previously been encountered [13–20].

We propose that these VLP may represent a new virus family that shares morphologic features with more than 1 viral family. It is highly unlikely that they represent different viruses because their associated ICI were identified using the same monoclonal antibody. It is not possible or judicious to use TEM images from suboptimally preserved autopsy tissue from only 3 cases to speculate on the viral family that may be involved. Future ultrastructural studies on better-preserved lung specimens are urgently needed.

Regarding preservation of lung and other tissues from autopsies, the time elapsed between death, autopsy, and specimen fixation are the critical factors [21]. Although glutaraldehyde fixation is the method of choice for TEM, 10% buffered formalin fixation is more than adequate, speed being the most critical factor. The actual preservation conditions for these 3 cases are not known, but TEM indicated that it was suboptimal. Therefore, it is encouraging that VLP were identified at all. With better-preserved tissue, it should be feasible to obtain much more definitive information on both the ICI and VLP.

Our hypothesis is that a ubiquitous, previously unidentified respiratory virus with limited homology at best to known viruses is responsible for KD in genetically predisposed children. Immunologic, histologic, electron microscopic, and RNA expression data support this hypothesis over a superantigen or an autoimmune etiology for the illness. Discovery of ''new viruses'' without significant homology to known viruses can be both technically challenging and labor-intensive [22]. As an example of the problem of detecting ''new'' viruses, we randomly chose a 100 bp sequence of hepatitis C virus nucleocapsid gene [ccggtgagta caccggaatc gccgggatga ccgggtcctt tcttggataa acccgctcaa tgcccggaaa tttgggcgtg cccccgcaag actgctagcc] and did BLAST searches limited to sequences that were not hepatitis C, to simulate a BLAST analysis of a new virus sequence prior to its entry into Genbank; no viral matches were identified.

We hope that this publication, suggesting the presence of a ''new'' virus associated with KD, will encourage physicians who care for patients with fatal KD and medical examiners trying to determine the cause of unexpected childhood deaths to be more aggressive in requesting autopsy permission for research, and performing expedited autopsies with the rapid fixation of lung tissue, using both formalin and 2.5% neutral-buffered glutaraldehyde. The lungs should be well-sampled to guarantee the presence of adequate numbers of medium sized bronchi. Confirmed or suspected KD deaths should undergo comprehensive autopsies that include samples of all organs and tissues, including as many arteries (especially, but not exclusively, the coronary arteries) as possible. In addition, tissue should be snap frozen for nucleic acid analyses including those using new and emerging molecular techniques [23]. We encourage a worldwide effort to obtain better tissue samples that could facilitate the identification of the etiologic agent of KD.

Supplementary Data

Supplementary data are available at http://jid.oxfordjournals.org online.

Funding

This work is supported by the National Institutes of Health (grants R01 HL63771 to A.H.R. and R21 HL089526 to S.C.B.), the Max Goldenberg Foundation, and the Kawasaki Disease Fund of the Children's Memorial Hospital.

References

1. Rowley AH, Baker SC, Orenstein JM, Shulman ST. Searching for the cause of Kawasaki disease–cytoplasmic inclusion bodies provide new insight. Nat Rev Microbiol **2008**; 6:394–401.
2. Rowley AH, Shulman ST, Spike BT, Mask CA, Baker SC. Oligoclonal IgA response in the vascular wall in acute Kawasaki disease. J Immunol **2001**; 166:1334–43.
3. Rowley AH, Baker SC, Shulman ST, et al. Detection of antigen in bronchial epithelium and macrophages in acute Kawasaki disease by use of synthetic antibody. J Infect Dis **2004**; 190:856–65.
4. Rowley AH, Baker SC, Shulman ST, et al. Cytoplasmic inclusion bodies are detected by synthetic antibody in ciliated bronchial epithelium during acute Kawasaki disease. J Infect Dis **2005**; 192:1757–66.
5. Rowley AH, Baker SC, Shulman ST, et al. RNA-containing cytoplasmic inclusion bodies in ciliated bronchial epithelium months to years after acute Kawasaki disease. PLoS One **2008**; 3:e1582.
6. Garcia-Mata R, Gao YS, Sztul E. Hassles with taking out the garbage: Aggravating aggresomes. Traffic **2002**; 3:388–96.
7. Johnston JA, Ward CL, Kopito RR. Aggresomes: A cellular response to misfolded proteins. J Cell Biol **1998**; 143:1883–98.
8. Yang ZP, Cummings PK, Patton DL, Kuo CC. Ultrastructural lung pathology of experimental *Chlamydia pneumoniae* pneumonitis in mice. J Infect Dis **1994**; 170:464–7.
9. Toivola DM, Strnad P, Habtezion A, Omary MB. Intermediate filaments take the heat as stress proteins. Trends Cell Biol **2010**; 20:79–91.
10. Rowley AH, Shulman ST, Garcia FL, et al. Cloning the arterial IgA antibody response during acute Kawasaki disease. J Immunol **2005**; 175:8386–91.
11. Chari R, Lonergan KM, Ng RT, MacAulay C, Lam WL, Lam S. Effect of active smoking on the human bronchial epithelium transcriptome. BMC Genomics **2007**; 8:297.
12. Komuro A, Bamming D, Horvath CM. Negative regulation of cytoplasmic RNA-mediated antiviral signaling. Cytokine **2008**; 43: 350–8.
13. Koenig S, Gendelman HE, Orenstein JM, et al. Detection of AIDS virus in macrophages in brain tissue from AIDS patients with encephalopathy. Science **1986**; 233:1089–93.
14. Orenstein JM, Jannotta F. Human immunodeficiency virus and papovavirus infections in acquired immunodeficiency syndrome: An ultrastructural study of three cases. Hum Pathol **1988**; 19:350–61.
15. Eilbott DJ, Peress N, Burger H, et al. Human immunodeficiency virus type 1 in spinal cords of acquired immunodeficiency syndrome patients with myelopathy: Expression and replication in macrophages. Proc Natl Acad Sci USA **1989**; 86:3337–41.
16. Orenstein JM. Ultrastructural pathology of human immunodeficiency virus infection. Ultrastruct Pathol **1992**; 16:179–210.
17. Orenstein JM, Alkan S, Blauvelt A, et al. Visualization of human herpesvirus type 8 in Kaposi's sarcoma by light and transmission electron microscopy. AIDS **1997**; 11:F35–45.
18. Orenstein JM. Isn't a picture still worth a thousand words? Ultrastruct Pathol **2000**; 24:67–74.
19. Orenstein JM. Human endogenous retroviral expression by leukocytes. Ultrastruct Pathol **2000**; 24:123–4.
20. Orenstein JM. Replication of HIV-1 in vivo and in vitro. Ultrastruct Pathol **2007**; 31:151–67.
21. Graham L, Orenstein JM. Processing tissue and cells for transmission electron microscopy in diagnostic pathology and research. Nat Protoc **2007**; 2:2439–50.
22. Wu Q, Luo Y, Lu R, et al. Virus discovery by deep sequencing and assembly of virus-derived small silencing RNAs. Proc Natl Acad Sci USA **2010**; 107:1606–11.
23. Rowley AH. Finding the cause of Kawasaki disease: a pediatric infectious diseases research priority. J Infect Dis **2006**; 194:1635–7.